Small molecules efficiently reprogram apical papilla stem cells into neuron-like cells

QIXIN CHEN[1,2*], CHANGYONG YUAN[2*], SHAN JIANG[1], BOON CHIN HENG[3], TING ZOU[1], ZHONGSHAN SHEN[4], PENGLAI WANG[2] and CHENGFEI ZHANG[1]

[1]Restorative Dental Sciences, Endodontology, Faculty of Dentistry, The University of Hong Kong, Hong Kong 999077, SAR; [2]Department of Implant Dentistry, The Affiliated Stomatological Hospital of Xuzhou Medical University, Xuzhou, Jiangsu 221002; [3]School of Stomatology, Peking University, Beijing 100081; [4]Jiangsu Province Key Laboratory of Anesthesia and Analgesia Application Technology, Xuzhou Medical University, Xuzhou, Jiangsu 221004, P.R. China

Received November 5, 2019; Accepted September 8, 2020

DOI: 10.3892/etm.2021.9978

Abstract. Stem cell-based therapy may provide a novel approach for neural tissue regeneration. A small molecule cocktail-based culture protocol was previously shown to enhance neurogenic differentiation of stem cells from dental tissues. The present study aimed to investigate the early phase of small molecule-induced neurogenic differentiation of stem cells from the apical papilla (SCAP). SCAP were cultured in neural-induction medium or neural-induction medium with small molecules (NIMS-SCAP) and examined for their cell morphologies. Expression levels of neural progenitor cell-related markers, including Nestin, paired-box gene 6 (Pax6) and Sry-related HMG box 2 (Sox2), were examined using western blotting and immunocytofluorescence. Expression of differentiated neuron-related markers, including neurofilament protein (NFM), neuron-specific nuclear protein (NeuN) and microtubule-associated protein (MAP)-2, were also examined using western blotting, while NFM and MAP2 gene expression and cell proliferation were assessed using reverse transcription-quantitative (RT-q)PCR and Cell Counting Kit (CCK)-8 assays, respectively. SCAP morphology was affected by small molecules after as little as 30 min. Specifically, Nestin, Pax6 and Sox2 expression detected using western blotting was increased by day 3 but then decreased over the course of 7 days with neural induction, while immunocytofluorescence revealed expression of all three markers in NIMS-SCAP. The protein levels of NFM, NeuN and MAP2 on day 7 were significantly upregulated in NIMS-SCAP, as detected using western blotting, while NFM and MAP2 gene expression levels detected using RT-qPCR were significantly increased on days 5 and 7. Proliferation of NIMS-SCAP ceased after 5 days. Electrophysiological analysis showed that only SCAP cultured in NIMS had the functional activity of neuronal cells. Thus, small molecules reprogrammed SCAP into neural progenitor cells within the first 3 days, followed by further differentiation into neuron-like cells.

Correspondence to: Professor Penglai Wang, Department of Implant Dentistry, The Affiliated Stomatological Hospital of Xuzhou Medical University, 130 Huaihai West Road, Xuzhou, Jiangsu 221002, P.R. China
E-mail: wpl0771@163.com

Professor Chengfei Zhang, Restorative Dental Sciences, Endodontology, Faculty of Dentistry, The University of Hong Kong, 34 Hospital Road, Sai Ying Pun, Hong Kong 999077, SAR, P.R. China
E-mail: zhangcf@hku.hk

*Contributed equally

Abbreviations: CCK-8, Cell Counting Kit-8; iPSCs, induced pluripotent stem cells; MAP2, microtubule-associated protein 2; MSCs, mesenchymal stem cells; NeuN, neuron-specific nuclear protein; NFM, neurofilament protein; NPCs, neural progenitor cells; Pax6, paired-box gene 6; RT-qPCR, reverse transcription-quantitative polymerase chain reaction; Sox2, Sry-related HMG box 2, TTX, tetrodotoxin; TEA, tetraethyl ammonium

Key words: small molecule, stem cells, apical papilla, differentiation, neurogenesis

Introduction

Neural diseases and injuries, such as intracerebral hemorrhage, spinal cord injuries and peripheral nerve injuries, may be life-threatening, and often have detrimental impacts on patients' daily life and work activities (1-3). Various treatment strategies, including pharmacotherapy and surgery, have been investigated; however, effective strategies are still lacking due to inconsistent clinical benefits (1-3). Stem cell-based transplantation therapy has notable therapeutic potential, but acquisition of an adequate, ready-to-use stem cells for transplantation remains a major challenge. Neural progenitor (NPCs)/stem cells derived from aborted human fetuses and cadavers may be ideal candidates, but it is impossible to obtain a sufficient number of transplantable cells for clinical applications. Furthermore, although human embryonic stem cells possess a high tendency for neural differentiation, the ethical issues limit their clinical application (4). Neural-lineage

cells can easily differentiate from induced pluripotent stem cells (iPSCs), but the use of retroviruses to generate iPSCs causes safety concerns on retroviral DNA integration into the host cell genome (5). Mesenchymal stem cells (MSCs) isolated from bone marrow and adipose tissues also exhibit some neurogenic differentiation potential (6-9), but procuring MSCs from patients requires invasive surgical procedures, and the neurogenic potential of these cells is limited.

Dental tissue-derived stem cells have high neurogenic potential because of their embryonic neural crest origin, and may represent an alternative cell source for neuroregeneration (10). Furthermore, some dental stem cells were shown to express pluripotency markers like NANOG and OCT4 that are not usually expressed in other MSCs (11,12), and their neuroregenerative potential has been corroborated by *in vivo* studies on stroke (13) and neurodegenerative diseases (14). Dental stem cells can be easily collected from extracted teeth, cryopreserved and thawed when required. Stem cells from apical papilla (SCAP) with strong survival in harsh environments and high proliferative capacity represent excellent seed cells for tissue engineering (15). In previous studies, SCAP transplanted into the injured spinal cord or sciatic nerve significantly improved nerve regeneration and exerted neuroprotective effects (16,17).

It was reported that small molecules could drive the neural reprogramming of somatic cells (18). A previous study applied the same small molecule cocktail used by Hu *et al* (18) and successfully enhanced the differentiation of dental pulp stem cells, SCAP and gingiva-derived MSCs into neural-lineage cells within 14 days, and a longer induction period leads to lower proliferation of the cells (19). Therefore, the present study aimed to optimize this induction period. Secondly, due to neural crest origin, SCAP are considered to be more amenable to reprogramming into neural-lineage cells compared with human fibroblasts (10,20). To the best of our knowledge, the present study was the first to investigate the early phase of SACP differentiation into neurons. Based on the aforementioned studies, 7 days was chosen as the induction period. It was hypothesized that small molecules, including valproic acid (VPA), CHIR99021, Repsox, forskolin, SP600125, GO6983 and Y-27632, may exert rapid effects on the neurogenic differentiation of SCAP, and that this process may differ from that observed in human fibroblasts (18). The present study investigated the differentiation of SCAP into neural-lineage cells within 7 days of treatment with small molecules.

Materials and methods

Culture of SCAP. Human SCAP were gifted by Dr Anibal Diogenes (Department of Endodontics, University of Texas Health Science Center at San Antonio, TX, USA) (21). Cells were seeded in α-minimum essential medium (α-MEM) containing 10% (v/v) fetal bovine serum and 1% (v/v) penicillin-streptomycin antibiotic solution (all Thermo Fisher Scientific, Inc.). Cultures were maintained at 37˚C in a 5% CO_2 incubator. The culture medium was changed every 2-3 days, and cells were subcultured when they reached 80% confluence.

Neural induction of SCAP. SCAP were seeded onto 6-well culture plates at a density of 20,000 cells/cm^2. The neural-induction protocol used was based on a previous study (18) with some modifications, including shortening the culture duration from 8 to 7 days. When the SCAP reached 60% confluence, the medium was changed to neural-induction medium (NIM) comprising of DMEM/F12/Neurobasal A at 1:1 supplemented with 0.5% (v/v) N2, 1% (v/v) B27 (all Thermo Fisher Scientific, Inc.), 100 mM cAMP (Sigma-Aldrich; Merck KGaA) and 20 ng/ml basic fibroblast growth factor (Thermo Fisher Scientific, Inc.), in the absence or presence of the chemical cocktail VCRFSGY (0.5 mM VPA, 3 μM CHIR99021, 1 μM Repsox, 10 μM forskolin, 10 μM SP600125, 5 μM GO6983 and 5 μM Y-27632) (NIMS). All of these small molecules were obtained from Sigma-Aldrich; Merck KGaA. The culture medium was refreshed on day 3. Cells were examined using light microscopy at a magnification of x20 or harvested for western blotting, immunocytofluorescence, reverse transcription-quantitative (RT-q)PCR and electrophysiological assays.

Western blotting. Cells were lysed by adding M-PER solution (Thermo Fisher Scientific, Inc.) containing protease inhibitor cocktail 4˚C for 20 min. The resulting protein samples were quantified using a BCA kit (Thermo Fisher Scientific, Inc.). Equal amounts of protein (25 μg) were loaded per lane onto a 7.5% gel, resolved using SDS-PAGE and subsequently transferred onto Immun-Blot PVDF membranes (Cyvita). The membranes were blocked with 5% (w/v) skimmed milk for 1 h and incubated overnight at 4˚C with primary antibodies against Nestin (1:100; cat. no. ab105389; Abcam), paired-box gene 6 (Pax6; 1:1,000; cat. no. 60433; Cell Signaling Technology, Inc.), Sry-related HMG box 2 (Sox2; 1:1,000; cat. no. 3579S; Cell Signaling Technology, Inc.), neurofilament protein (NFM; 1:1,000; cat. no. RMO-270; Invitrogen; Thermo Fisher Scientific, Inc.), neuron-specific nuclear protein (NeuN; 1:1,000; cat. no. 702022; Invitrogen; Thermo Fisher Scientific, Inc.) and microtubule-associated protein 2 (MAP2; 1:500; cat. no. 13-1500; Invitrogen; Thermo Fisher Scientific, Inc.). After washing with Tris-buffered saline/0.1% Tween-20, the membranes were incubated with horseradish peroxidase-conjugated anti-mouse IgG or horseradish peroxidase-conjugated anti-rabbit IgG (both Cell Signaling Technology, Inc.) secondary antibodies for 2 h at room temperature. The antibody-antigen complexes were visualized using Pierce ECL Western Blotting Substrate (Thermo Fisher Scientific, Inc.). Relative densities quantified using ImageJ software (v1.6.0; National Institute of Health).

Immunocytofluorescence. Cells were fixed with 4% (v/v) paraformaldehyde at room temperature for 20 min, washed three times with phosphate-buffered saline (PBS), permeabilized with 0.5% (w/v) Triton X-100 for 5 min at 4˚C, and blocked in PBS containing 5% (w/v) bovine serum albumin (Sigma-Aldrich; Merck KGaA) at room temperature for 1 h. The fixed samples were incubated with primary antibodies against Nestin (1:100; cat. no. ab105389; Abcam), Pax6 (1:200; cat. no. 60433; Cell Signaling Technology, Inc.) and Sox2 (1:400; cat. no. 3579S; Cell Signaling Technology, Inc.) overnight at 4˚C. After removal of excess primary antibodies by washing with PBS, the samples were incubated with Alexa Fluor 488-conjugated goat anti-mouse or tetramethylrhodamine-conjugated goat

anti-rabbit (both Abcam) secondary antibodies for 1 h at room temperature in the dark, followed by washing with PBS. The cell nuclei were stained with DAPI for 5 min at room temperature and the samples were imaged by laser scanning microscopy (LSM710; Carl Zeiss AG) at x20 magnification at specific excitation/emission wavelengths for TRITC (540/570 nm) and Alexa Fluor 488 (490/520 nm).

RT-qPCR. Total RNA was extracted from cultured SCAP using an RNeasy Plus Mini kit (Qiagen, Inc.). The extracted RNA was reverse transcribed to cDNA using the SuperScript® VILO® Master Mix (Thermo Fisher Scientific, Inc.) according to the manufacturer's instructions. The reaction was incubated at 25˚C for 10 min, followed by 42˚C for 60 min, and terminated at 85˚C for 5 min. RT-qPCR was carried out using a StepOne Real-Time PCR system (Applied Biosystems; Thermo Fisher Scientific, Inc.) and SYBR™ Green Master Mix (Thermo Fisher Scientific, Inc.). The primer sequences for the neural markers are shown in Table I. The $2^{-\Delta\Delta Cq}$ method (22) was used to calculate the Cq-value for each gene and target gene expression levels were normalized to the housekeeping gene GAPDH. Analysis of all gene markers was repeated three times. RT-qPCR amplifications were carried out using the following parameters: 2 min At 50˚C, 20 sec at 95˚C, 40 cycles of 3 sec at 95˚C, 30 sec at 60˚C, 15 sec at 95˚C and 1 min at 60˚C.

Cell proliferation assay. SCAP were seeded into 96-well plates at a density of 10,000 cells/well and preincubated at 37˚C under 5% CO_2 for 24 h. The original culture medium was discarded and replaced with α-MEM, neural-induction medium or neural-induction medium with small molecules. The samples were analyzed on days 1, 3, 5 and 7 using a Cell Counting Kit (CCK)-8 cell proliferation assay kit (Dojindo Molecular Technologies, Inc.) according to the manufacturer's instructions. Briefly, CCK-8 solution (10 μl) was added to each well and incubated for 3 h at 37˚C under 5% CO_2. Subsequently, the absorbance was measured at 450 nm using a SpectraMax® M2 microplate reader (Molecular Devices, LLC).

Electrophysiological assay. Whole-cell patch-clamp recordings were conducted on the basis of a previously published method by Li *et al* (23). The cells were bathed with a solution containing (in mM): 145 NaCl, 1.5 KCl, 2 $CaCl_2$, 2 $MgCl_2$, 10 HEPES And 10 glucose (pH adjusted to 7.4 with NaOH). The patch-clamp pipettes had a resistance of 6-8 MΩ with an internal solution containing (in mM): 125 KCl, 1 $CaCl_2$, 2 $MgCl_2$, 2 Mg-ATP, 2 Na_2ATP, 10 HEPES And 10 EGTA (pH adjusted to 7.2 with KOH). The recordings were acquired using a A&M amplifier (Model 2400; A-M Systems, Inc.). Data were filtered at 4 kHz and analyzed with pCLAMP version 10.4 software (Axon Instruments). All experiments were performed at room temperature (22-25˚C). For voltage-clamp experiments, the cells were clamped at -80 mV for 400 ms and depolarized for 40 ms with voltage pulses from -80 to 200 mV at 20 mV intervals. Na^+ and K^+ current amplitudes were measured at the peak outward and inward values, respectively, and reported as current densities (pA/pF) for comparison. The Na^+ and K^+ currents were selectively blocked by 1 μM tetrodotoxin (TTX) and 35 mM tetraethyl ammonium (TEA), respectively. For current-clamp experiments, the cells were set at -80 mV holding potential, and the action potentials were elicited by step current injection of 100-300 pA for 1,000 ms.

Table I. Primer sequences utilized for RT-qPCR.

Gene	Primer sequence, 5'-3'
NFM	
Forward	GTCAAGATGGCTCTGGATATAGAAATC
Reverse	TACAGTGGCCCAGTGATGCTT
MAP2	
Forward	TTGGTGCCGAGTGAGAAGAA
Reverse	GGTCTGGCAGTGGTTGGTTAA
GAPDH	
Forward	TGCACCACCAACTGCTTAGC
Reverse	GGCATGGACTGTGGTCATGAG

NFM, neurofilament protein; MAP2, microtubule-associated protein 2.

Statistical analysis. All experiments were conducted in triplicate. Differences between SCAP were cultured in neural-induction medium (NIM-SCAP) and cultured in neural-induction medium with small molecules (NIMS-SCAP) were analyzed using an unpaired Student's t-tests, while differences among multiple cell groups were examined using a Tukeys post-hoc with a One-way ANOVA. The data were expressed as mean ± standard error of the mean. $P<0.05$ was considered to indicate a statistically significant difference. All statistical analyses were carried out using SPSS version 19.0 software (IBM Corp.).

Results

Morphological changes during neural induction. SCAP (Fig. 1A) were subjected to different neural-induction culture protocols over a period of 7 days. The cells were observed using phase-contrast light microscopy every 15-30 min during the first 12 h, and then on days 1, 3, 5 and 7. Morphological changes were discernible by 30 min in NIMS-SCAP (Fig. 1C), but only after 24 h in NIM-SCAP (Fig. 1D). The major initial changes included the appearance of an elongated morphology and bipolar neurites (Fig. 1C-K). NIMS-SCAP exhibited marked differences in cellular morphology compared with NIM-SCAP from days 1-7, including adoption of a rounded shape with a greater number of and longer neurite outgrowths after treatment with the small molecule cocktail. In contrast, NIM-SCAP mostly retained the morphological characteristics of MSCs, except for the appearance of neurites at the poles, with the entire cells being spindle-shaped. In addition, NIMS-SCAP neurites tended to become elongated until they connected with the neurites of adjacent cells.

Variation in the expression of NPC-related protein markers. The protein expression levels of NPC-related markers in NIM-SCAP and NIMS-SCAP were analyzed using western blotting on days 1, 3, 5 and 7 (Fig. 2A and B). Nestin, Pax6

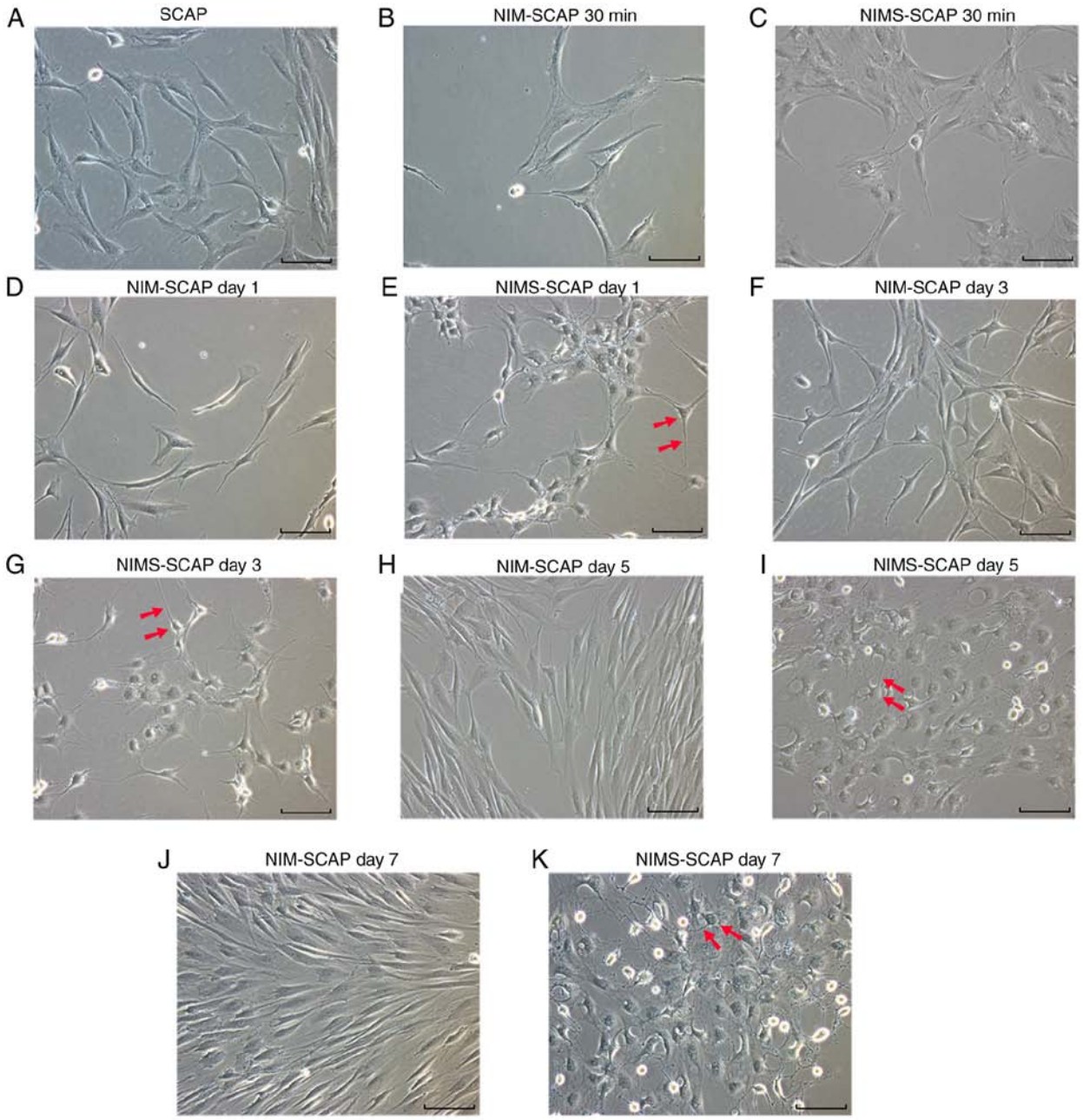

Figure 1. Morphological changes during neural induction. (A) SCAP morphology. NIM-SCAP morphology at (B) 30 min, days (D) 1, (F) 3, (H) 5 and (J) 7. NIMS-SCAP morphology at (C) 30 min, days (E) 1, (G) 3, (I) 5 and (K) 7. Scale bar, 100 μm; magnification, x20. Arrows, cell body and neurite. SCAP, apical papilla; NIM, neural-induction medium; NIMS, neural-induction medium with small molecules.

and Sox2 showed trends toward initial upregulation, followed by subsequent decreases, regardless of the presence of small molecules. In addition, all three NPC-related proteins peaked on day 3 under both neural-induction culture conditions. These results suggested that SCAP were induced into a NPC-like cell state at day 3, but that this state was unstable and short-lived, with the expression levels of NPC-related proteins decreasing over the following 4 days.

NPC-related protein expression during the NPC-like cell state. Both NIM-SCAP and NIMS-SCAP exhibited increased Nestin (Fig. 3A-C), Pax6 (Fig. 3D-F) and Sox2 (Fig. 3G-I) expression on day 3 compared with undifferentiated SCAP, according to qualitative immunocytofluorescence analysis. Nestin was expressed relatively strongly in SCAP, and thus there were minimal differences in the staining intensities compared with NIM-SCAP and NIMS-SCAP. Meanwhile, immunofluorescence staining of Pax6 and Sox2 was strongly enhanced in NIM-SCAP and NIMS-SCAP after induction, most notably Sox2 expression in NIMS-SCAP.

Expression of differentiated neuron-related markers. NFM, NeuN and MAP2 expression levels were significantly upregulated in NIMS-SCAP compared with NIM-SCAP (Fig. 4B-D, respectively), while these differentiated neuron markers were hardly detectable in undifferentiated SCAP (Fig. 4A). The gene expression levels of the neuron markers in NIM-SCAP and NIMS-SCAP were analyzed on days 1, 3, 5 and 7 using

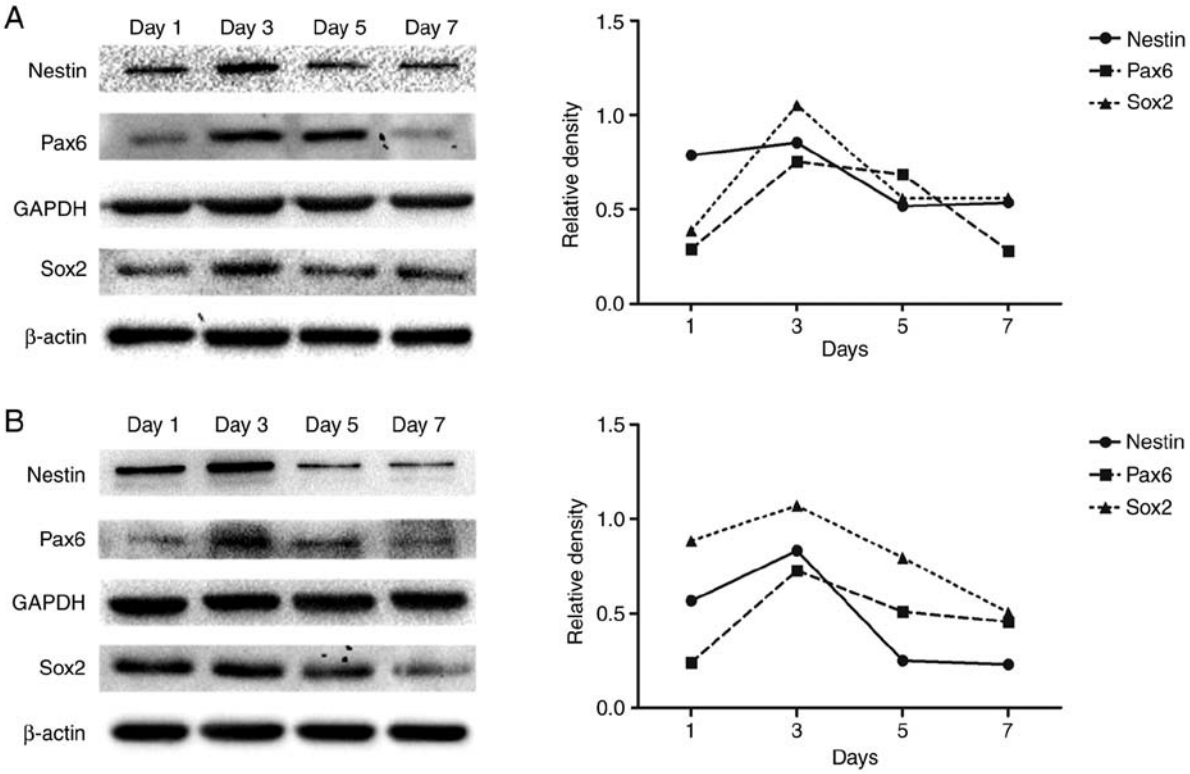

Figure 2. Variation in the expression of NPC-related protein markers. (A) Detection of Nestin, Pax6 and Sox2 protein expression levels in NIM-SCAP by western blotting on days 1, 3, 5 and 7. Corresponding line plots show the relative densities normalized to GAPDH (Nestin and Pax6) or β-actin (Sox2) as endogenous controls. (B) Detection of Nestin, Pax6 and Sox2 protein expression levels in NIMS-SCAP by western blotting on days 1, 3, 5 and 7. Corresponding line plots show the relative densities normalized to GAPDH (Nestin and Pax6) or β-actin (Sox2) as endogenous controls. SCAP, apical papilla; NIM, neural-induction medium; NIMS, neural-induction medium with small molecules; NPC, neural progenitor cell; Pax6, paired-box gene 6; Sox2, Sry-related HMG box 2.

RT-qPCR (Fig. 4E and F). NFM and MAP2 gene expression levels were signifincantly increased on days 1-5 in both NIM-SCAP and NIMS-SCAP. NFM expression continued to increase until day 7 in NIMS-SCAP, while MAP2 expression peaked on day 5 and was decreased on day 7, but remained higher compared with that on day 3. Meanwhile, NFM and MAP2 gene expression levels were only slightly increased in NIM-SCAP. NFM and MAP2 gene expression levels were significantly higher in NIMS-SCAP compared with NIM-SCAP on both days 5 and 7.

Cell proliferation assay. NIMS-SCAP proliferated more slowly compared with NIM-SCAP and SCAP, as evaluated using CCK-8 assays, but there were no significant differences in proliferation of SCAP, NIM-SCAP and NIMS-SCAP on days 1 and 3 (Fig. 5). Undifferentiated SCAP proliferated rapidly from days 3-5, while the proliferation rates of NIM-SCAP and NIMS-SCAP slowed down. The proliferation rate was slowest in NIMS-SCAP and the proliferation had ceased by day 7. Some cells failed to survive until day 7.

Electrophysiological functions. The cells that had a neuron-like morphology were selected. Whole-cell patch-clamp studies were performed to measure the voltage-dependent Na^+ and K^+ currents in the cells. The results indicated that there were voltage-dependent Na^+ and K^+ currents in NIMS-SCAP (Na^+ currents 18/45, K^+ currents 16/45), and not in NIM-SCAP and SCAP (Fig. 6A and B). The inward Na^+ currents were reversibly blocked by 1 μM TTX and rapidly recovered with washing off TTX (Fig. 6C and D). Similarly, the outward K^+ current was reversibly blocked by 35 mM TEA and rapidly recovered with washing off TEA (Fig. 6E and F). A single action potential (AP) was observed in a subset of NIMS-SCAP (n=3; AP 5/45; Fig. 6G), without any observed spontaneous AP activity during the current clamp experiments.

Discussion

A select combination of small molecules has been shown to reprogram human dermal fibroblasts into MSCs (24), and to reprogram mouse fibroblasts into NPCs (25), functional neurons (26), cardiomyocytes (27) and endothelial cells (28). Chemical-based strategies, which avoid the use of viral vectors, transgenic manipulation or gene modification, represent safe methods for the generation of clinically relevant cell lineages for regenerative transplantation and disease treatment (29-31). Furthermore, small molecules can exert transient, reversible and dose-dependent effects on the targeted cells, thereby allowing the timing and dosage to be precisely controlled and fine-tuned (29). Chemical-based approaches therefore represent a new paradigm and viable alternative to gene-based approaches for cell reprogramming.

A diverse variety of small-molecule chemicals have previously been utilized for cellular reprogramming (30-34). These chemicals can be divided into several categories based on their effects on cell physiology and signaling pathways: Histone deacetylase inhibitors, such as VPA; signaling pathway inhibitors, such as inhibitors of transforming growth factor (TGF)-β

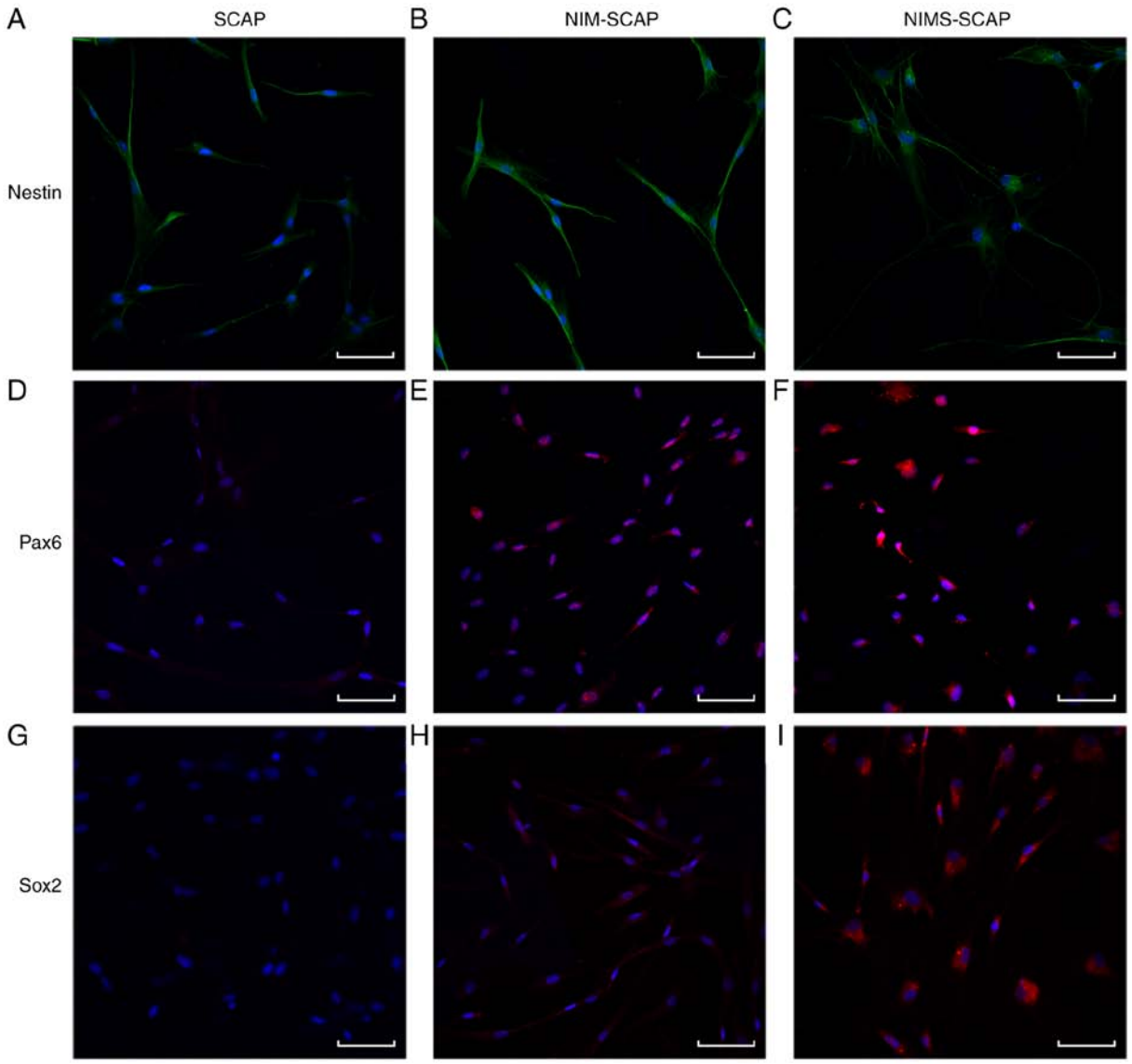

Figure 3. NPC-related protein expression during the NPC-like cell state. (A-C) Immunocytofluorescence for detection of Nestin expression in SCAP, NIM-SCAP and NIMS-SCAP at day 3. (D-F) Immunocytofluorescence for detection of Pax6 expression in SCAP, NIM-SCAP and NIMS-SCAP at day 3. (G-I) Immunocytofluorescence for detection of Sox2 expression in SCAP, NIM-SCAP and NIMS-SCAP at day 3. Nuclei were counterstained with DAPI (blue). Scale bar, 100 μm; magnification, x200. SCAP, apical papilla; NIM, neural-induction medium; NIMS, neural-induction medium with small molecules; NPC, neural progenitor cell; Pax6, paired-box gene 6; Sox2, Sry-related HMG box 2.

signaling (Repsox), glycogen synthase kinase (GSK)-3β (CHIR99021), protein kinase C (GO6983) and ROCK (Y-27632) and adenylate cyclase activators, such as forskolin, and SP600125, which was reported to improve the reprogramming efficiency of overexpressed exogenous transcription factors (35). Therefore, the present study examined the effect of the chemical cocktail VCRFSGY (0.5 mM VPA, 3 μM CHIR99021, 1 μM Repsox, 10 μM forskolin, 10 μM SP600125, 5 μM GO6983, 5 μM Y-27632) on SCAP reprogramming.

Changes in cell morphology were observed as early as 30 min after application of the small molecules, compared with no changes until 24 h in the NIM-SCAP. The morphology of NIM-SCAP remained similar to that of SCAP for the first 7 days of neural-induction culture, with some residual adult MSCs memory. In contrast to this, NIMS-SCAP were rapidly transformed into a neural-like phenotype with a larger number of and longer neurite outgrowths that became connected to one another to form a web-like network. Y-27632 was reported to promote neurite outgrowth in olfactory ensheathing cells (OECs) by inhibiting the Rho-associated coiled-coil-containing protein kinase (ROCK)/F-actin pathway Rho-associated protein kinase signaling pathway, and TGF-β1 shortened the length of the neurites and decreased cell elongation (36). In addition, TGF-β1 treatment reprogrammed OECs into a flattened morphology (37). In the present study, the effects of Repsox on the TGF-β signaling specifically were not demonstrated. Repsox is a known inhibitor of the TGF-β1 signaling pathway, therefore it was hypothesized that this inhibitor contributed to the enhanced neurite outgrowth and elongation of NIMS-SCAP in the present study.

NPCs, as a nascent neural-lineage cell type, can usually be identified by the expression of upstream neural markers, such as Nestin (38), Pax6 (39) and Sox2 (40). The present study

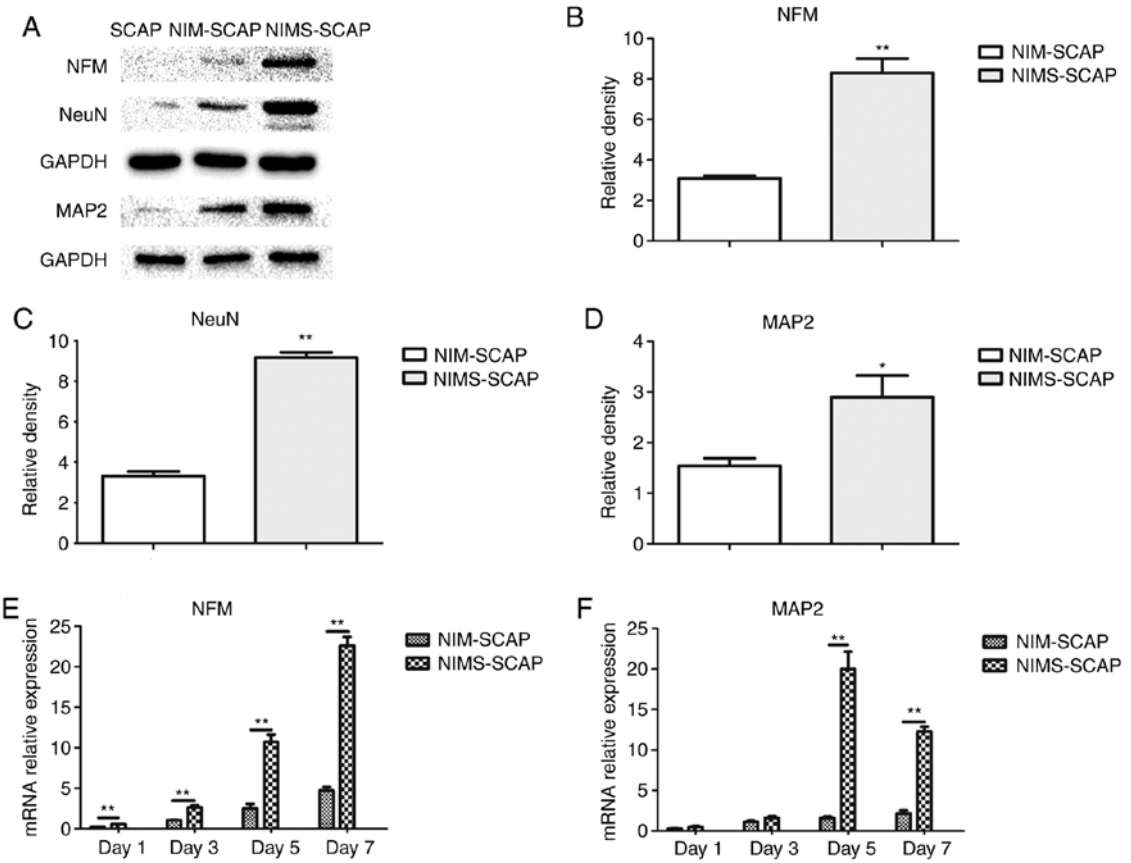

Figure 4. Expression of differentiated neuron-related markers. (A) Detection of NFM, NeuN and MAP2 protein expression levels in SCAP, NIM-SCAP and NIMS-SCAP on day 7 using western blotting. Relative densities quantified using ImageJ for (B) NFM (n=3), (C) NeuN (n=3) and (D) MAP2 (n=3). (E) NFM gene expression levels in NIM-SCAP and NIMS-SCAP on days 1, 3, 5 and 7 determined using RT-qPCR (n=6). (F) MAP2 gene expression levels in NIM-SCAP and NIMS-SCAP on days 1, 3, 5, and 7 determined by RT-qPCR (n=6). All data normalized to SCAP, which were assigned an arbitrary value of 1. *P<0.05, **P<0.01. NFM, neurofilament protein; NeuN, neuron-specific nuclear protein; MAP2, microtubule-associated protein 2; SCAP, apical papilla; NIM, neural-induction medium; NIMS, neural-induction medium with small molecules; RT-qPCR, reverse transcription-quantitative PCR.

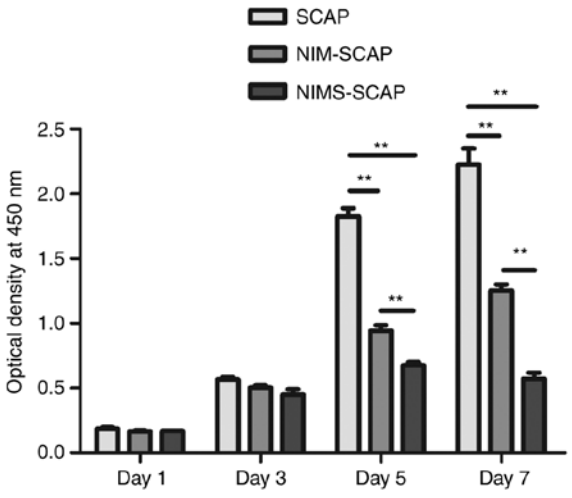

Figure 5. Cell proliferation of SCAP, NIM-SCAP and NIMS-SCAP determined using Cell Counting Kit-8 assays. n=3. **P<0.01. SCAP, apical papilla; NIM, neural-induction medium; NIMS, neural-induction medium with small molecules.

demonstrated time-dependent changes in the expression of these NPC-related proteins in NIM-SCAP and NIMS-SCAP, with increases during the early phase of neural induction followed by subsequent downregulation. These results suggested that SCAP may be induced by small molecules into an NPC-like cell state by day 3, followed by further differentiation into neuron-like cells. The NPC self-renewal marker Nestin (38) was expressed at a lower level in NIMS-SCAP compared with NIM-SCAP, suggesting that NIMS-SCAP progressed to a more mature neural stage more rapidly. The immunocytofluorescence results revealed that Sox2 expression was more prominent in NIMS-SCAP compared with in NIM-SCAP or SCAP. Both VPA and GO6983 have previously been shown to induce cells into a more plastic state (30,32), while Sox2 expression levels in iPSCs treated with VPA were similar to those in embryonic stem cells (30). Moreover, VPA, Repsox and CHIR99021 inhibited histone deacetylases, while TGF-β and GSK-3 activated the expression of endogenous Sox2 (25,30,41-43). In contrast to the present results, the immunostaining analysis reported Hu *et al* (18), who formulated the small molecule cocktail-based induction protocol used in the present study, showed no expression of neural progenitor markers (Nestin, Pax6 or Sox2) during the induction procedure. These differences may be due to the cell types used in both studies, for example SCAP have higher neurogenic potential compared with human fibroblasts (10). Even without any neural induction, SCAP can also express Nestin due to its neural crest origin (10).

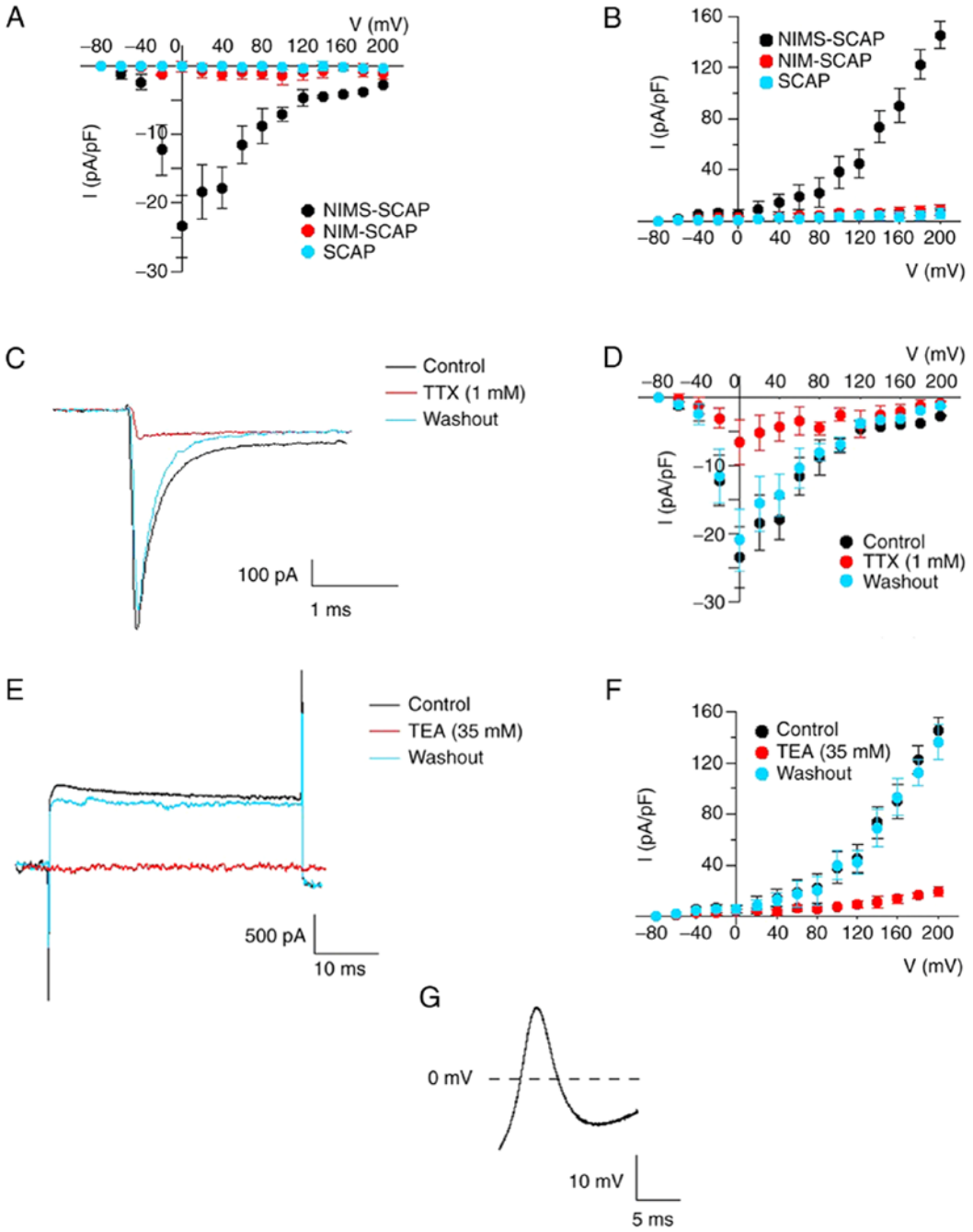

Figure 6. Electrophysiology of NIMS-SCAP. (A) I-V relationship of Na^+ currents from -80 to 200 mV on NIMS-SCAP (n=6), NIM-SCAP (n=6) and SCAP (n=6). (B) I-V relationship of K^+ currents from -80 to 200 mV on NIMS-SCAP (n=6), NIM-SCAP (n=6) and SCAP (n=6). (C and D) Perfusion on NIMS-SCAP of 1 μM TTX reversibly blocked Na^+-inward currents (n=6). (E and F) Perfusion on NIMS-SCAP of 35 mM TTX reversibly blocked K^+-outward currents (n=6). (G) Trace showing 300 pA input current for 1,000 ms induced action potential waveform in the NIMS-SCAP. SCAP, apical papilla; NIM, neural-induction medium; NIMS, neural-induction medium with small molecules; TTX, tetrodotoxin; TEA, tetraethyl ammonium.

In the present study, the expression levels of neural progenitor markers continued to decline on days 5-7, therefore it was hypothesized that the induced SCAP were progressing further along the neural differentiation pathway. The expression levels of differentiated neural markers in the cells were compared on day 7 using western blotting. NFM, NeuN and MAP2, as markers of differentiated neurons (44-46), were significantly upregulated, demonstrating that the small molecules dramatically accelerated neural-lineage differentiation. There was a consistent increase in gene expression in NIMS-SCAP on days 1-5, and NFM expression was detected up to day 7. MAP2 expression declined on day 7 compared with day 5; however, it remained at a much higher level compared with that in NIM-SCAP. Previously, the combination of GSK-3β inhibition (CHIR99021) and adenylate cyclase signaling activation (forskolin) has been shown to improve neuronal reprogramming efficiency (47), and CHIR99021 and Repsox increases the neuronal conversion of human fibroblasts via overexpression of Achaete-scute homolog 1 and neurogenin 2 (31). In the present study, small

molecules dramatically decreased the duration required for differentiation into neural-lineage cells.

The proliferation of NIMS-SCAP slowed significantly on day 5 compared with that of NIM-SCAP, as shown by the CCK-8 assays. Moreover, some cells failed to survive until day 7. Taken together with the presence of differentiated neuron markers, these results suggested that stemness was decreased after 5 days of induction with small molecules, thus preventing stem/progenitor cells from undergoing self-renewal and proliferation, given that neurons are highly differentiated and mitotically inactive cells (19). In contrast to the present results, Hu *et al* (18) found that the majority of induced neuronal cells survived for 10-12 days, which could suggest that differentiated neuron-like cells are in a mitotically inactive state after small-molecule induction.

Besides morphological changes and upregulation of protein and gene expression, the most important characteristics of neuron is its electrophysiological activities (23). The result of whole-cell patch-clamp studies revealed that NIMS-SCAP resulted in voltage-dependent Na^+ and K^+ currents, which were blocked by TTX and TEA and restored after the blocker was washed away. Moreover, a single action potential was observed. These results suggested that some of the cells have been transformed into mature neurons. These results were consistent with previous studies reporting that dental-derived stem cells differentiated into neuron-like cells (23,48). In previous studies, neurosphere culture was used to promote the neurogenic differentiation of cells, which is also widely utilized as a classical method to induce and amplify neural lineage cells (25,49). By using the method of neurosphere culture, neuron maturation takes ~1 month (23), while induction by small molecules significantly reduces the time for neuron differentiation to have electrophysiological functions. The combination of small molecules and neurosphere culture can identify spontaneous cell postsynaptic currents (23).

In summary, the present study demonstrated that small molecules can rapidly induce SCAP into an NPC-like state, which are then easily differentiated into neuron-like cells. Cell proliferation decreased in line with the downregulation of NPC-related marker expression and ceased by day 5, indicating that differentiated neuron-like cells had been generated. This was the first study to efficiently induce SCAP into NPC. The translational application of NPC derived from SCAP for nerve regeneration and repair needs to be further studied by animal models.

Acknowledgements

Not applicable.

Funding

This work was funded by The Health and Medical Research Fund (Hong Kong) - Full Grant (grant no. 06172396; to CZ).

Availability of data and materials

The datasets used and/or analyzed during the current study are available from the corresponding author on reasonable request.

Authors' contributions

PW and CZ designed the experiments. QC, SJ, TZ and ZS performed the experiments. QC, CY and PW analyzed the data. QC and BCH analyzed the data and wrote the manuscript. CY, PW, and CZ revised the manuscript. All authors read and approved the final manuscript.

Ethics approval and consent to participate

Not applicable.

Patient consent for publication

Not applicable.

Competing interests

The authors declare that they have no competing interests.

References

1. Wilkinson DA, Pandey AS, Thompson BG, Keep RF, Hua Y and Xi G: Injury mechanisms in acute intracerebral hemorrhage. Neuropharmacology 134: 240-248, 2018.
2. Hurlbert RJ, Hadley MN, Walters BC, Aarabi B, Dhall SS, Gelb DE, Rozzelle CJ, Ryken TC and Theodore N: Pharmacological therapy for acute spinal cord injury. Neurosurgery 72 (Suppl 2): S93-S105, 2013.
3. Panagopoulos GN, Megaloikonomos PD and Mavrogenis AF: The present and future for peripheral nerve regeneration. Orthopedics 40: e141-e156, 2017.
4. McComish SF and Caldwell MA: Generation of defined neural populations from pluripotent stem cells. Philos Trans R Soc Lond B Biol Sci 373: 20170214, 2018.
5. Chambers SM, Fasano CA, Papapetrou EP, Tomishima M, Sadelain M and Studer L: Highly efficient neural conversion of human ES and iPS cells by dual inhibition of SMAD signaling. Nat Biotechnol 27: 275-280, 2009.
6. Wang Y, Li ZW, Luo M, Li YJ and Zhang KQ: Biological conduits combining bone marrow mesenchymal stem cells and extracellular matrix to treat long-segment sciatic nerve defects. Neural Regen Res 10: 965-971, 2015.
7. Zhao H, Cheng L, Du X, Hou Y, Liu Y, Cui Z and Nie L: Transplantation of cerebral dopamine neurotrophic factor transducted BMSCs in contusion spinal cord injury of rats: Promotion of nerve regeneration by alleviating neuroinflammation. Mol Neurobiol 53: 187-199, 2016.
8. Georgiou M, Golding JP, Loughlin AJ, Kingham PJ and Phillips JB: Engineered neural tissue with aligned, differentiated adipose-derived stem cells promotes peripheral nerve regeneration across a critical sized defect in rat sciatic nerve. Biomaterials 3: 242-251, 2015.
9. Hsueh YY, Chang YJ, Huang TC, Fan SC, Wang DH, Chen JJ, Wu CC and Lin SC: Functional recoveries of sciatic nerve regeneration by combining chitosan-coated conduit and neurosphere cells induced from adipose-derived stem cells. Biomaterials 35: 2234-2244, 2014.
10. Parisi L and Manfredi E: Applicability of tooth derived stem cells in neural regeneration. Neural Regen Res 11: 1704-1707, 2016.
11. Lima RL, Holanda-Afonso RC, Moura-Neto V, Bolognese AM, DosSantos MF and Souza MM: Human dental follicle cells express embryonic, mesenchymal and neural stem cells markers. Arch Oral Biol 73: 121-128, 2017.
12. Athanassiou-Papaefthymiou M, Papagerakis P and Papagerakis S: Isolation and characterization of human adult epithelial stem cells from the periodontal ligament. J Dent Res 94: 1591-1600, 2015.
13. Yamagata M, Yamamoto A, Kako E, Kaneko N, Matsubara K, Sakai K, Sawamoto K and Ueda M: Human dental pulp-derived stem cells protect against hypoxic-ischemic brain injury in neonatal mice. Stroke 44: 551-554, 2013.

14. Shamir C, Venugopal C and Dhanushkodi A: Dental pulp stem cells for treating neurodegenerative diseases. Neural Regen Res 10: 1910-1911, 2015.
15. Huang GT, Sonoyama W, Liu Y, Liu H, Wang S and Shi S: The hidden treasure in apical papilla: The potential role in pulp/dentin regeneration and bioroot engineering. J Endod 34: 645-651, 2008.
16. De Berdt P, Vanacker J, Ucakar B, Elens L, Diogenes A, Leprince JG, Deumens R and des Rieux A: Dental apical papilla as therapy for spinal cord injury. J Dent Res 94: 1575-1581, 2015.
17. Kolar MK, Itte VN, Kingham PJ, Novikov LN, Wiberg M and Kelk P: The neurotrophic effects of different human dental mesenchymal stem cells. Sci Rep 7: 12605, 2017.
18. Hu W, Qiu B, Guan W, Wang Q, Wang M, Li W, Gao L, Shen L, Huang Y, Xie G, *et al*: Direct conversion of normal and Alzheimer's disease human fibroblasts into neuronal cells by small molecules. Cell Stem Cell 17: 204-212, 2015.
19. Heng BC, Jiang S, Yi B, Gong T, Lim LW and Zhang C: Small molecules enhance neurogenic differentiation of dental-derived adult stem cells. Arch Oral Biol 102: 26-38, 2019.
20. Alt E, Yan Y, Gehmert S, Song YH, Altman A, Gehmert S, Vykoukal D and Bai X: Fibroblasts share mesenchymal phenotypes with stem cells, but lack their differentiation and colony-forming potential. Biol cell 103: 197-208, 2011.
21. Ruparel NB, de Almeida JF, Henry MA and Diogenes A: Characterization of a stem cell of apical papilla cell line: Effect of passage on cellular phenotype. J Endod 39: 357-363. 2013.
22. Livak KJ and Schmittgen TD: Analysis of relative gene expression data using real-time quantitative PCR and the 2(-Delta Delta C(T)) method. Methods 25: 402-408, 2001.
23. Li D, Zou XY, El-Ayachi I, Romero LO, Yu Z, Iglesias-Linares A, Cordero-Morales JF and Huang GT: Human dental pulp stem cells and gingival mesenchymal stem cells display action potential capacity in vitro after neuronogenic differentiation. Stem Cell Rev Rep 15: 67-81, 2019.
24. Lai PL, Lin H, Chen SF, Yang SC, Hung KH, Chang CF, Chang HY, Lu FL, Lee YH, Liu YC, *et al*: Efficient generation of chemically induced mesenchymal stem cells from human dermal fibroblasts. Sci Rep 7: 44534, 2017.
25. Cheng L, Hu W, Qiu B, Zhao J, Yu Y, Guan W, Wang M, Yang W and Pei G: Generation of neural progenitor cells by chemical cocktails and hypoxia. Cell Res 24: 665-679, 2014.
26. Cheng L, Gao L, Guan W, Mao J, Hu W, Qiu B, Zhao J, Yu Y and Pei G: Direct conversion of astrocytes into neuronal cells by drug cocktail. Cell Res 25: 1269-1272, 2015.
27. Fu Y, Huang C, Xu X, Gu H, Ye Y, Jiang C, Qiu Z and Xie X: Direct reprogramming of mouse fibroblasts into cardiomyocytes with chemical cocktails. Cell Res 25: 1013-1024, 2015.
28. Sayed N, Wong WT, Ospino F, Meng S, Lee J, Jha A, Dexheimer P, Aronow BJ and Cooke JP: Transdifferentiation of human fibroblasts to endothelial cells: Role of innate immunity. Circulation 131: 300-309, 2015.
29. Xie M, Cao N and Ding S: Small molecules for cell reprogramming and heart repair: Progress and perspective. ACS Chem Biol 9: 34-44, 2014.
30. Huangfu D, Maehr R, Guo W, Eijkelenboom A, Snitow M, Chen AE and Melton DA: Induction of pluripotent stem cells by defined factors is greatly improved by small-molecule compounds. Nat Biotechnol 26: 795-797, 2008.
31. Ladewig J, Mertens J, Kesavan J, Doerr J, Poppe D, Glaue F, Herms S, Wernet P, Kögler G, Müller FJ, *et al*: Small molecules enable highly efficient neuronal conversion of human fibroblasts. Nat Methods 9: 575-578, 2012.
32. Gafni O, Weinberger L, Mansour AA, Manor YS, Chomsky E, Ben-Yosef D, Kalma Y, Viukov S, Maza I, Zviran A, *et al*: Derivation of novel human ground state naive pluripotent stem cells. Nature 504: 282-286, 2013.
33. PLOS ONE Staff: Correction: Neurotrophic requirements of human motor neurons defined using amplified and purified stem cell-derived cultures. PLoS One 10: e0119195, 2015.
34. Liu ML, Zang T, Zou Y, Chang JC, Gibson JR, Huber KM and Zhang CL: Small molecules enable neurogenin 2 to efficiently convert human fibroblasts into cholinergic neurons. Nat Commun 4: 2183, 2013.
35. Zhu S, Ambasudhan R, Sun W, Kim HJ, Talantova M, Wang X, Zhang M, Zhang Y, Laurent T, Parker J, *et al*: Small molecules enable OCT4-mediated direct reprogramming into expandable human neural stem cells. Cell Res 24: 126-129, 2014.
36. Li Y, Huo S, Fang Y, Zou T, Gu X, Tao Q and Xu H: ROCK inhibitor Y27632 induced morphological shift and enhanced neurite outgrowth-promoting property of olfactory ensheathing cells via YAP-dependent up-regulation of L1-CAM. Front Cell Neurosci 12: 489, 2018.
37. Li Y, Zou T, Xue L, Yin ZQ, Huo S and Xu H: TGF-β1 enhances phagocytic removal of neuron debris and neuronal survival by olfactory ensheathing cells via integrin/MFG-E8 signaling pathway. Mol Cell Neurosci 85: 45-56, 2017.
38. Bernal A and Arranz L: Nestin-expressing progenitor cells: Function, identity and therapeutic implications. Cell Mol Life Sci 75: 2177-2195, 2018.
39. Sakayori N, Kikkawa T and Osumi N: Reduced proliferation and excess astrogenesis of Pax6 heterozygous neural stem/progenitor cells. Neurosci Res 74: 116-121, 2012.
40. Han DW, Tapia N, Hermann A, Hemmer K, Höing S, Araúzo-Bravo MJ, Zaehres H, Wu G, Frank S, Moritz S, *et al*: Direct reprogramming of fibroblasts into neural stem cells by defined factors. Cell Stem Cell 10: 465-472, 2012.
41. Ichida JK, Blanchard J, Lam K, Son EY, Chung JE, Egli D, Loh KM, Carter AC, Di Giorgio FP, Koszka K, *et al*: A small-molecule inhibitor of TGF-beta signaling replaces sox2 in reprogramming by inducing nanog. Cell Stem Cell 5: 491-503, 2009.
42. Li W, Zhou H, Abujarour R, Zhu S, Young Joo J, Lin T, Hao E, Schöler HR, Hayek A and Ding S: Generation of human-induced pluripotent stem cells in the absence of exogenous Sox2. Stem Cells 27: 2992-3000, 2009.
43. Maherali N and Hochedlinger K: Tgfbeta signal inhibition cooperates in the induction of iPSCs and replaces Sox2 and cMyc. Curr Biol 19: 1718-1723, 2009.
44. Steinschneider R, Delmas P, Nedelec J, Gola M, Bernard D and Boucraut J: Appearance of neurofilament subunit epitopes correlates with electrophysiological maturation in cortical embryonic neurons cocultured with mature astrocytes. Dev Brain Res 95: 15-27, 1996.
45. Weyer A and Schilling K: Developmental and cell type-specific expression of the neuronal marker NeuN in the murine cerebellum. J Neurosci Res 73: 400-409, 2003.
46. Soltani MH, Pichardo R, Song Z, Sangha N, Camacho F, Satyamoorthy K, Sangueza OP and Setaluri V: Microtubule-associated protein 2, a marker of neuronal differentiation, induces mitotic defects, inhibits growth of melanoma cells, and predicts metastatic potential of cutaneous melanoma. Am J Pathol 166: 1841-1850, 2005.
47. Pfisterer U, Ek F, Lang S, Soneji S, Olsson R and Parmar M: Small molecules increase direct neural conversion of human fibroblasts. Sci Rep 6: 38290, 2016.
48. Gervois P, Struys T, Hilkens P, Bronckaers A, Ratajczak J, Politis C, Brône B, Lambrichts I and Martens W: Neurogenic maturation of human dental pulp stem cells following neurosphere generation induces morphological and electrophysiological characteristics of functional neurons. Stem Cells Dev 24: 296-311, 2015.
49. Zhang Q, Nguyen PD, Shi S, Burrell JC, Xu Q, Cullen KD and Le AD: Neural crest stem-like cells non-genetically induced from human gingiva-derived mesenchymal stem cells promote facial nerve regeneration in rats. Mol Neurobiol 55: 6965-6983, 2018.